The Effects of Disk Morphology on Flying-Height Modulation: Experiment and Simulation

Brian H. Thornton, D. B. Bogy
Computer Mechanics Laboratory
Dept. of Mechanical Engineering
University of California
Berkeley, CA. 94720

C. S. Bhatia
IBM/SSD
5600 Cottle Road
San Jose, CA. 95193

Abstract – ***The effect of morphology on flying height modulation (FHM) of a sub-10 nm flying air bearing slider was studied for three different disks by experiment and simulation. The experimental measurement methods are discussed and a new single beam laser Doppler vibrometer (LDV) measurement method, which yielded the highest resolution with a 2 mm beam spot size, was introduced. Analysis was performed in three different frequency bandwidths – a geometric FHM from 10 kHz to 100 kHz, a dynamically excited FHM from 100 kHz to 500 kHz and the third being negligible compared to the other two bands, above 500 kHz. Transfer function analysis was carried out to investigate the FHM in the lowest frequency band. FHM in the first band was shown to be caused primarily by a phase shift between the sliders' response and the disks' morphology and secondarily by decreasing slider motion with decreasing morphology wavelength, which correlated well with previous work. For two of the disks investigated, the FHM due to the disks' morphology showed air bearing excitation that resulted in an intolerable level of FHM. However, for one of the disks studied, the FHM was as low as the disk morphology for wavelengths of 2 mm and less, which was within tolerable limits. It is concluded that when designing a disk for low FHM, it is not sufficient to characterize the quality of a disk by a single number such as roughness or waviness. Proper design and optimization of both the disk and air bearing slider results in FHM that is lower than the disks' morphology.***

I. Introduction

With flying-heights (FH) decreasing as magnetic areal density increases a better understanding of the dynamics at the head-disk interface (HDI) is required. There are numerous parameters, the effects of some of which are still unknown, that affect the tribological and magnetic performance at the HDI. The condition of "steady" flying, or flying without contact, over an actual magnetic disk at sub-10 nm FH is not yet completely understood. But understanding the dynamics of the slider due to the disk morphology is required for the design of a stable HDI. The physical spacing requirement for 100 Gbit/in^2 data density is only 6 nm at the transducer location [3]-[4]. Also, reliable reading and writing of magnetic data requires that the transducer location on the slider fluctuate by no more than ±10 % of the nominal FH, which means ±0.6 nm [4]. An accurate method for measuring FHM due to repeatable events such as disk morphology and other motions of the disk was proposed previously by Zeng *et al.* [1].

We applied the LDV to measure FHM in a manner similar to that proposed by Zeng *et al.* with a slight modification [1]. The modification entailed a single or absolute measurement of the disk and slider with a smaller, 2 μm, beam diameter in order to improve spatial resolution. It was found that not only was a higher resolution obtained, but also we were better able to directly compare experimental and simulation results. In this way we investigated three different "super-smooth" disks with an air bearing slider that was designed for 100 Gbit/in^2 applications. By keeping the other experimental conditions constant, we compared the FHM of the three disks experimentally and by simulation. Excellent agreement between the experimental and simulation results was found. Analysis of the data was broken into three distinct frequency bandwidths: Band I:

10 kHz to 100 kHz, Band II: 100 kHz to 500 kHz, and Band III: greater than 500 kHz. It was shown that the FHM amplitude in Band I, which was found to be the geometric FHM, was on the same order as the disk morphology. The FHM in Band II was found to be dominated by the dynamics of the air bearing slider. It was shown that for a certain level of disk morphology, the air bearing was excited to an intolerable level of FHM. In Band III, it was found that the slider had essentially zero absolute motion as the disk morphology passed underneath. However, the FHM in Band III could be neglected as compared to that in Bands I and II due to the low amplitude of the disk roughness at such high frequencies. From this study, we conclude that many factors need to be taken into consideration when designing a "steady" flying slider and a reliable HDI. With proper design of both the air bearing surface (ABS) and the disk, small fluctuations in the FH can be obtained yielding a more reliable HDI at sub-10 nm spacing, and these fluctuations can be held within ±10 %.

II. EXPERIMENTAL SETUP

The experimental results shown in this paper were obtained using a modification of the experimental setup explained in detail by Zeng *et al*. [1]. A Thôt Technologies platform with the flyability option was the basic test stand. We used a Polytec LDV with a highpass filter set at 20 kHz for triggering at a small radial scratch on the outer diameter of the disk. This ensures accurate triggering for averaging the measurement. A Polytec 512 LDV with a highpass filter at 5kHz was used for the actual measurement of the disk and slider motion. Data acquisition was accomplished using a LeCroy oscilloscope sampled at 5 MHz and averaged 500 times. All data post-processing was carried out using Matlab. This general testing platform has shown at least 95 % repeatability for measurements on the nanometer scale [1].

A. Single LDV Beam Measurement Technique

Instead of using a LDV differential beam measurement as in Zeng *et al.* [1], we used a single LDV beam for absolute motion measurement with a beam spot size of approximately 2 μm. However, this can only be accomplished using the velocity output mode of the LDV. The necessary dynamic resolution would be lost if the displacement mode of the LDV were utilized.

As a disk spins, its morphology, clamping distortions, warpage, and other repeatable motions, as viewed by a stationary slider, can be decomposed into an infinite sum of sinusoids having different amplitudes, A_i, frequencies, w_i, and phases, f_i:

$$d(t) = \sum_{i=1}^{\infty} A_i \sin(w_i t + f_i) \qquad (1)$$

The velocity, v(t) of this displacement is:

$$v(t) = \sum_{i=1}^{\infty} A_i w_i \cos(w_i t + f_i) \qquad (2)$$

Displacement can be recovered by numerical integration of the velocity. Generally, for "super-smooth" disks, the amplitudes of the components decay exponentially as the frequency increases. If the displacement output mode were used with the LDV, the low frequency content of the disk morphology would overwhelm the higher frequency content, yielding low resolution across the bandwidth. The amplitudes of the velocity components are $A_i\omega_i$ which can be thought of as an exponentially decaying function, *A(w)*, multiplied by linear increasing ω. This helps maintain a higher resolution across the wide bandwidth of interest.

Several comparisons between differential and single beam measurements and different beam spot sizes were completed. Beam spot sizes of approximately 20 μm, 10 μm, and 2 μm were used. However, for the differential dual beam measurement, one of the beams could be no smaller than 20 μm due to the optics arrangement on the tester. For a given sampling frequency, f_s, the spatial resolution of the disk is v/f_s, where v is the relative linear velocity between the slider and the disk. For the test case presented in this paper with f_s equal to 5 MHz, the spatial resolution was 3.7 μm/sample. If the beam spot size were greater than the spatial resolution, the disk morphology resolution would be lost. Figure 1 shows time domain plots of the FHM and Table 1 contains peak-to-peak and 3σ values of the FHM for different measurement methods of the same HDI system. Differential or dual beam and single beam measurements of the FHM for beam sizes of 10 μm and 2 μm are shown (recall that in the dual beam measurement one beam was 20 μm). The 20 μm beam was the limiting factor of resolution for the dual beam method. It can be seen that the peak-to-peak and standard deviation values increase slightly as the beam size decreases. This is due to the ability to capture more high frequency components or very small wavelength features on the disk surface. By using the single beam or absolute measurement not only was higher resolution obtained but also a better understanding could be inferred from the results, as will be seen later in the paper. This measurement technique provides the absolute motion of the disk surface under the slider as well as the absolute motion of the slider. By subtraction of these measurements the FHM can be obtained.

B. Effects of Disk Morphology on FHM

A comparison of three different "super-smooth" disks under the same experimental conditions with the same slider was conducted. Skew angle was set to zero. The linear velocity of 18.7 m/s was chosen to be 1-2 m/s faster than that associated with the first signs of contact, determined by the LDV velocity response of the slider, between the roughest disk and the slider. When the frequency content of the signal contains torsion and/or bending modes of the slider body, at 1.25 MHz and 1.65 MHz, respectively, it is assumed that contact has occurred. Even though the nominal FH of the slider was the same for all three disks, the clearance over the high spots and asperities of the disks were different. The slider under investigation was a pico negative-pressure symmetric design with a 1.5 gm preload and with the ABS shown in Fig. 2.

The transducer FH at the test conditions was approximately 9 nm. The slider chosen for the experiment had good agreement in its attitude parameters (FH, pitch and roll) between measurements on a Phase Metrics Dynamic Flying-Height Tester and simulation using the Computer Mechanics Laboratory (CML) Air Bearing Design Code. The LDV beam was positioned on the slider body adjacent to the transducer to obtain the FHM at the transducer location for comparison between experiment and simulation. The band of the digital filter was from 10 kHz to 2 MHz.

III. EXPERIMENTAL RESULTS

The three disks investigated, disks A, B, and C are labeled in decreasing order of waviness and roughness. Figure 3 shows the frequency content of the disk morphologies from 10 kHz to 2 MHz plotted in nanometers on log-linear axes. When investigating FHM due to disk morphology, we must consider the spectral content of the entire bandwidth. Disks A and B had glass substrates and disk C had an aluminum substrate. As can be seen from Fig. 3, the manufacturing processes and substrates can have an effect on surface characteristics. Figure 4 shows the frequency content of the FHM obtained from the three different disks. By comparing Fig. 3 to Fig. 4, we observe that the FHM for disk C appears to be the same as the disk morphology. Also, comparison of the results for disks A and B, shows excitations of the air bearing modes at approximately 160 kHz and 320 kHz, which causes large fluctuations.

IV. COMPARISION: EXPERIMENT AND SIMULATION

Simulations were performed using the CML Dynamic Air Bearing Simulator. The measured disk morphologies were used as the input data for the disk surface topographies for the simulator. This one-dimensional measurement was extended radially across the disk surface in the simulation, as a rough approximation of the two-dimensional morphology. For this specific case where the ABS is symmetric, the transducer is at the center of the trailing edge, and the skew is zero degrees, the error from this approximation is expected to be minimized.

Figure 5 shows the experimentally measured disk morphology of disk C that was used in the simulation. The comparison between the FHM from experiment and simulation for disk C are shown in Fig. 6, where excellent correlation is seen. Similar results were obtained for the other two disks. A summary of the results for all three disks is shown in Table 2. The percentages shown in Table 2 are the peak-to-peak FHM normalized by the nominal FH, which for this case was 9 nm. Also, shown in Table 2 are the 3σ values of the FHM found experimentally, which were close to those values found by simulation. Excellent correlation of experiment and simulation was found for both time and frequency domain comparisons. From Table 2, it can be seen that for disk C, the FHM stays within the tolerable ±10 %, yielding ±5.8 % and ±7.35 % for experimental and simulation, respectively. However, disks A and B exceed this criteria drastically yielding ±37 % and ±20.2 % from the experimental results, respectively.

V. DISCUSSION

The three disks under investigation have very different morphologies as seen from Fig. 3. The effect of the morphology on FHM can now be analyzed using both the experimental and simulation results. We analyzed the data in three distinct frequency bandwidths: Band I: 10 kHz < f < 100 kHz, Band II: 100 kHz < f < 500 kHz, and Band III: f > 500 kHz, where f is frequency. The experimentally determined standard deviations (σ) of the disk morphologies and FHMs are shown in each frequency band for all three disks in Fig. 7. Figure 8 presents the ratio of the standard deviation of the FHM to the standard deviation of the disk morphology, broken into Bands I, II, and III for disks A, B, and C. The ratios in Fig. 8 are outputs (FHM) divided be the inputs (disk morphology) showing the "gain" of the system in the different frequency bands for the three disks.

Band I corresponds to the geometric FHM [2]. Geometric FHM occurs at frequencies below the modal frequencies of the air bearing slider that are determined by the geometry of the ABS, pressure profile underneath the ABS and the disk morphology [2]. This is a complicated function and for this particular ABS, the geometric FHM was on the same order as the disk morphology in Band I [2]. As seen from Figs. 7 and 8, this holds true for all three disks investigated.

Band II spans the modal frequencies of the air bearing slider. If we consider the air film and slider to be a linear system for small perturbations (which is not true for large perturbations) under the condition of "steady" flying, the air bearing modal frequencies for the ABS under investigation fall within Band II. So in Band II, the disk morphologies excite this dynamical system and cause a resonance type FHM. Two modes are excited when the slider flies over disks A and B. The differences in the frequency peaks in Fig. 4 for disks A and B have to do with the differences in the clearance between the disk and the slider. For disk A the clearance was less than for disk B, causing the air bearing modal stiffness to increase. These two modes are the first and second pitch modes of the air bearing. The roll mode does not contribute to FHM at the transducer due to the symmetry of the ABS and the transducer location. From Figs. 4, 7, 8, and Table 2 it is apparent that for disks A and B there was an excessive level of excitation of the air bearing, causing FHM. However, for disk C, the disk morphology is so low in amplitude that the air bearing was not excited and actually shows a FHM that is lower in amplitude than the disk morphology in Band II. From Fig. 8, the gain of the FHM to the disk displacement was more than 2 for disks A and B, but it was only approximately 1 for disk C. From Fig. 3, it can be seen that in Band II, the FHM amplitude for disk C decreases with frequency much faster than for the other two disks. The results show how sensitive the FHM is to air bearing excitation. Different air bearing slider designs will have different threshold values for excitation due to the disk morphology.

Band III covers the high frequency range in which the disk morphology passes underneath the slider without causing any real absolute motion. It is also seen from Figs. 3 and 7, that the amplitudes of the disk morphologies in Band III were negligible for all three disks, compared to those in Bands I and II.

A. Explanation of Band I

Even in HDIs where the air bearing dynamics are not excited (i.e. the case for disk C, see Fig. 7), there may still be a high level of FHM due to the geometric effect mentioned earlier. This effect has been explained in detail in the numerical simulation investigation [2]. The geometric effect is due to a phase shift between the disk surface topography and the response at the transducer location on the slider and also a decrease in the absolute motion of the slider as the wavelength on the disk decreases. This was shown numerically using a sinusoidal waviness on the disk with various wavelengths but not for an actual disk surface that is composed of an infinite number of sinusoids over all frequencies, as seen in equation (1) [2]. If we use transfer function analysis to decompose the ratio of the output (slider motion) to the input (disk surface motion) into amplitude and phase verses frequency we can compare the experiment and simulation for the response to an actual disk. We used the Welch's averaged periodogram numerical method for estimating the transfer function between the disk and the slider motions with the aid of Matlab. Figures 9 and 10 show the estimated transfer functions for the experimental and simulation results for both amplitude and phase. Instead of plotting the transfer function verses frequency, f, it was plotted verses wavelength, λ, on the disk: λ =

v/f. In Fig. 10, it is seen that the phase relationship of the ratio of slider motion to that of the disk, for both the experimental and simulation, is similar to that seen in [2]. Similarly, from Fig. 9 it can be seen that the amplitude of the absolute motion of the slider decreases as the disk waviness wavelength decreases. Both of these effects combined cause the geometric FHM, but the phase shift is the primary cause and the decrease in the slider vibration amplitude is a secondary cause [2].

VI. Summary And Conclusion

In this study, we modified an existing experimental method to measure the FHM and obtained an increase in resolution, more insight into the mechanics, and as a result we were able to make direct comparisons between experiment and simulation. Different LDV beam sizes were used and compared, showing that the highest resolution was obtained with the single beam measurement using the smallest beam size of 2 μm. Experiments were conducted to obtain the FHM over three different disks. Using the measured disk topographies we obtained a direct comparison between experiment and simulation that showed excellent correlation. The FHM was analyzed using the experiments and simulations in the time and frequency domains. Three distinct frequency bandwidths were used to analyze of the effect of disk morphology on FHM. Band I: 10 kHz < f < 100 kHz was the band of the geometric FHM. Additional analysis in this bandwidth using transfer function analysis correlated the results obtained here with previous findings from simulations [2]. The geometric FHM amplitude for the particular system studied was on the same order as the disk morphology. However, depending on the slider ABS design and the disk morphology, this geometric FHM may be greater or less than the disk morphology [2]. The FHM in frequency Band II: 100 kHz < f < 500 kHz was influenced by the dynamics of the air bearing. If the disk morphology amplitude in Band II is low enough, excitation of the air bearing does not contribute to the FHM due to the disk morphology. The FHM in frequency Band III: 500 kHz < f < 2 MHz was so low that it could be neglected compared to Bands I and II. It is obvious that a single number characterization of roughness or waviness is not sufficient to determine the quality of a disk with respect to FHM. We have shown that, for the particular slider used with disk C, the FHM amplitude is on the order of the disk morphology. However, optimization can be achieved with both the ABS design and the disk morphology to obtain an even lower FHM. Also, with the correlation realized here between experiment and simulation, simulations can now be used as a design tool. New ABS designs can be modeled and simulated for FHM due to disk morphology prior to manufacturing.

ACKNOWLEDGMENT

This work was supported by The Computer Mechanics Laboratory at the University of California, Berkeley, USA and the National Storage Industry Consortium (NSIC).

REFERENCES

[1] Q.H. Zeng, B.H. Thornton, D.B. Bogy, and C.S Bhatia, "Flyability and Flying Height Modulation Measurement of Sliders with Sub-10nm Flying Heights," IEEE Trans. on Mag., Vol. 37, No.2, pp. 894-899, March 2001.

[2] B.H. Thornton, A. Nayak, and D.B. Bogy, "Flying Height Modulation Due to Disk Waviness of Sub-5nm Flying Height Air Bearing Sliders," J. of Tribology, submitted for publication

[3] T Pitchford, "Head/Disk Interace Tribology Measurements for 100Gb/in^2," Proceedings of the Symposium on Interface Technology Towards 100 Gbit/in^2, ASME, TRIB-Vol. 9, pp. 83-90, 1999.

[4] A. Menon, "Critical Requirements for 100Gb/in^2 Head/Media Interface," Proceedings of the Symposium on Interface Technology Towards 100 Gbit/in^2, ASME, TRIB-Vol. 9, pp. 1-9, 1999.

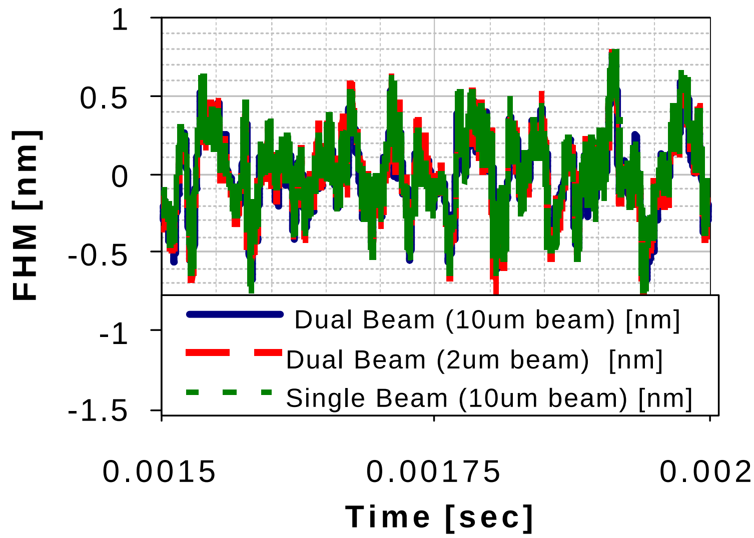

Fig. 1: FHM comparison between dual beam and single beam LDV measurements.

	Dual Beam (10μm beam size)	Dual Beam (2μm beam size)	Single Beam (10μm beam size)	Single Beam (2μm beam size)
Peak-to-Peak FHM [nm]	1.72	1.93	1.93	2.05
3σ [nm]	0.78	0.82	0.82	0.87

Table 1: Peak-to-peak and 3s values of FHM for different measurement methods.

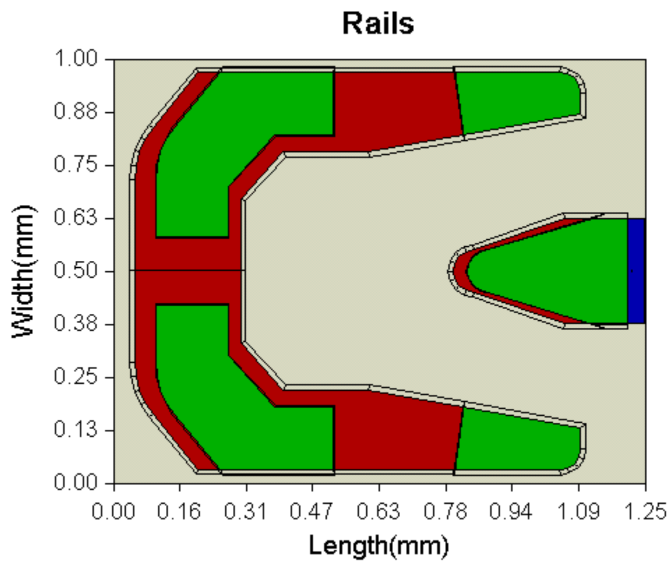

Fig. 2: 100 Gbit/in^2 ABS design.

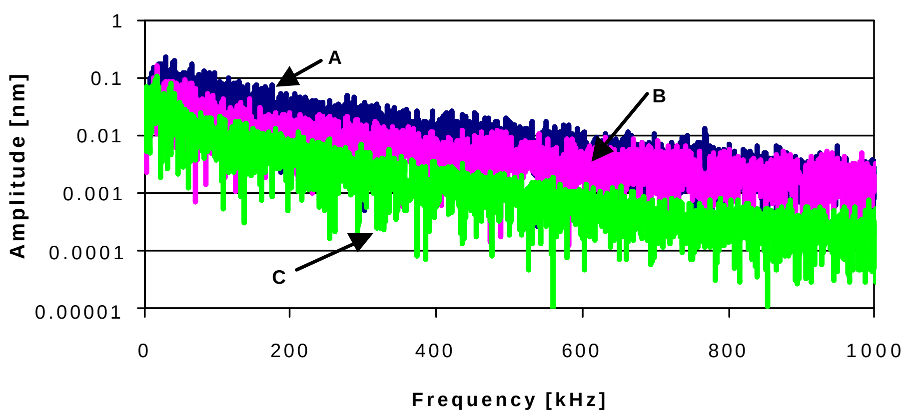

Fig. 3: Power spectral density of disks A, B and C morphologies as seen from a stationary point as the disk rotates.

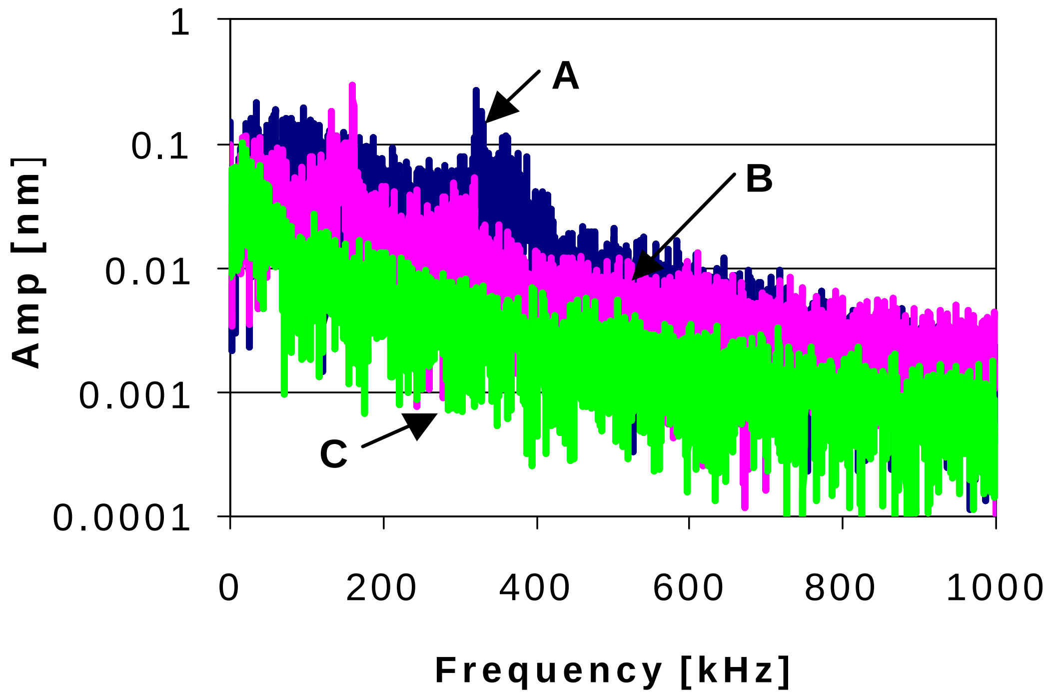

Fig. 4: Power spectral density of the FHM at the transducer location for disks A, B, and C.

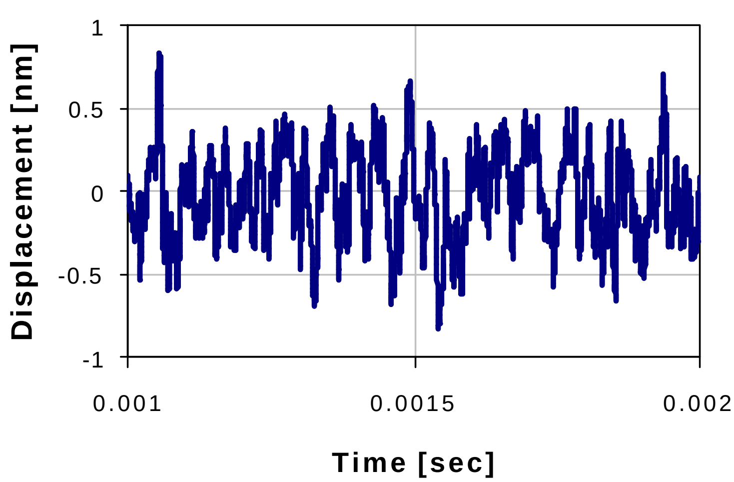

Fig. 5: Measured disk morphology of disk C used in the simulation.

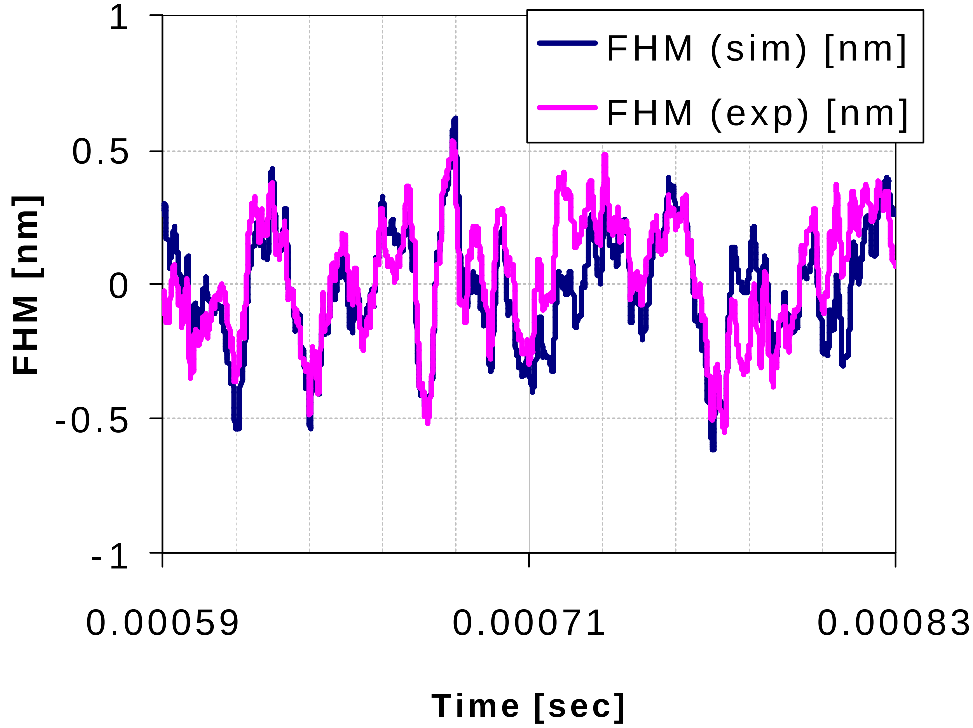

Fig. 6: Comparison of experiment and simulation of the FHM for disk C.

	Disk A	Disk B	Disk C
Experimental FHMp-p/FHnom	74%	40.4%	11.6%
Simulation FHMp-p/FHnom	60%	38%	14.7%
Experimental 3σ [nm]	5.04	2.43	0.81

Table 2: The ratio of FHM peak-to-peak to the nominal FH for disks A, B, and C found experimentally and by simulation. Also, 3s of FHM found experimentally.

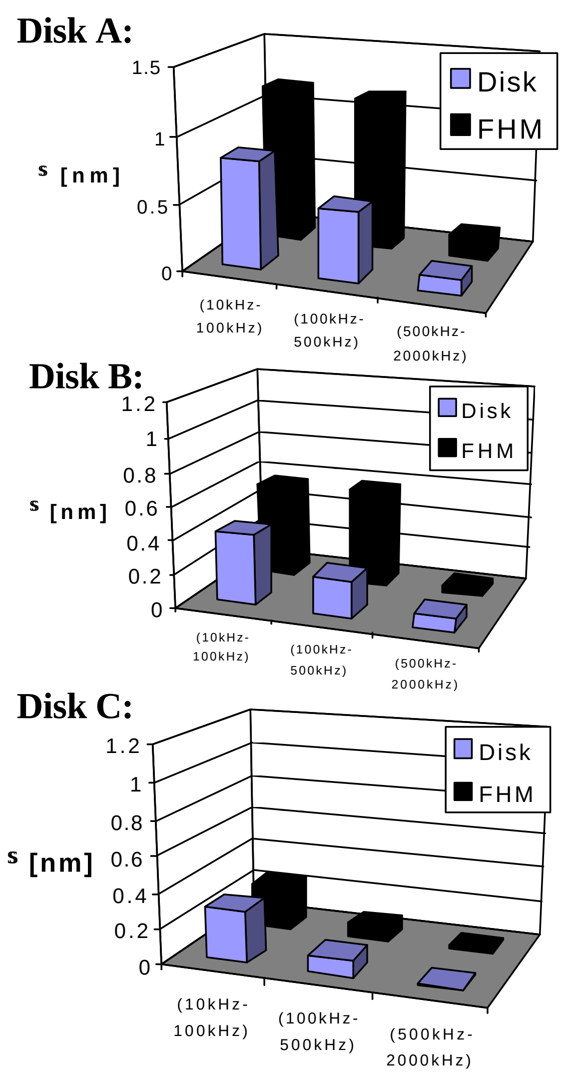

Fig. 7: Standard deviation of disk morphologies and FHM for disks A, B and C broken into the three Bands; Band I: 10kHz-100kHz, Band II: 100kHz-500kHz and Band III: >500kHz.

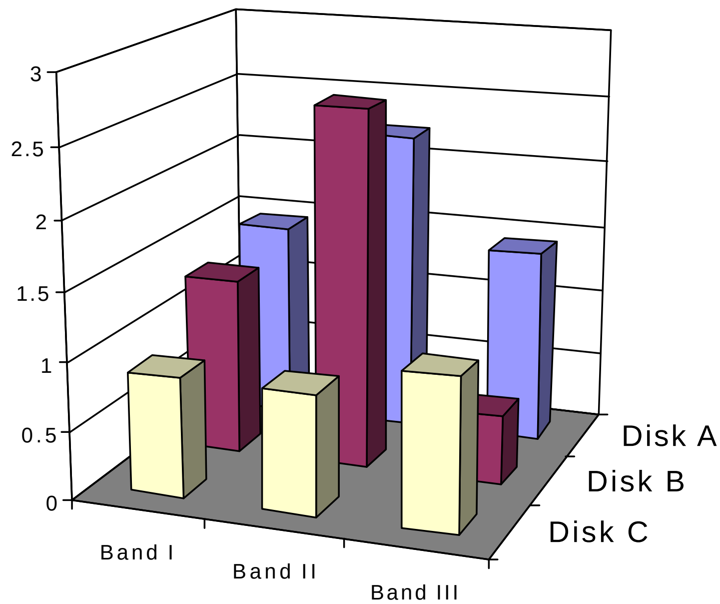

Fig. 8: Ratio of the standard deviation of FHM to the disk morphology broken into different Bands for disks A, B, and C.

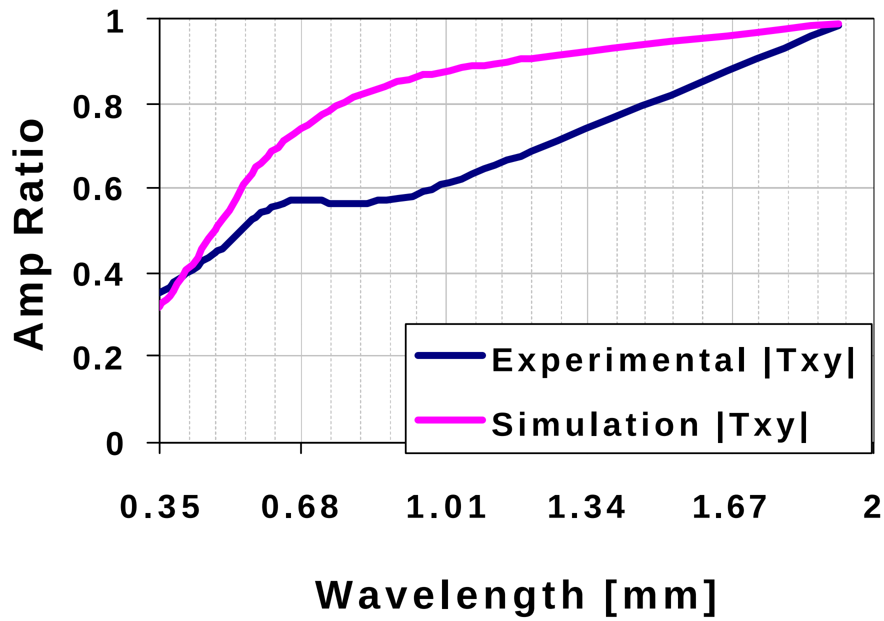

Fig. 9: Amplitude ratio of the slider to the disk displacement as a function of wavelength on the disk morphology.

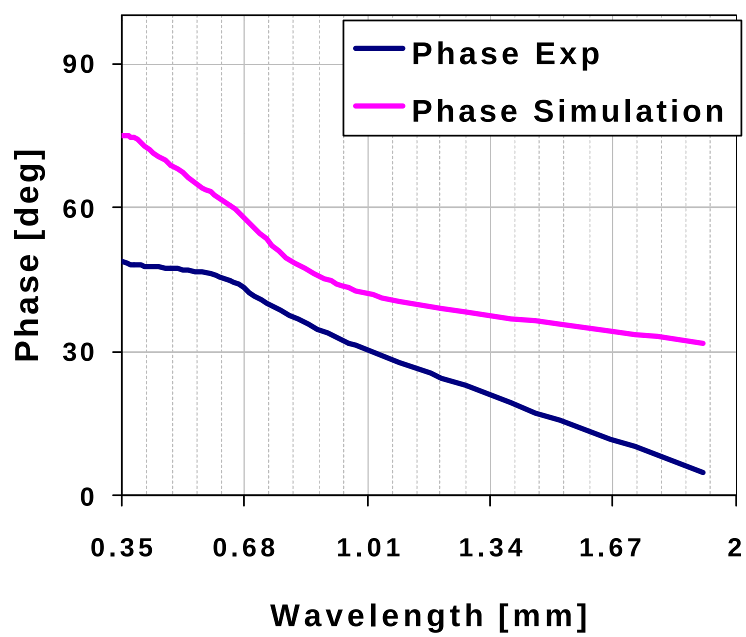

Fig. 10: Phase shift between the sliders displacement to that of the disk.